JOURNAL OF CATALYSIS **166,** 388–392 (1997)
ARTICLE NO. CA971513

NOTE

The V^{4+}/V^{5+} Balance as a Criterion of Selection of Vanadium Phosphorus Oxide Catalysts for *n*-Butane Oxidation to Maleic Anhydride: A Proposal to Explain the Role of Co and Fe Dopants

Vanadium phosphorous oxide catalysts (VPO) are well known for the oxidation of *n*-butane to maleic anhydride, and many papers and patents have been published in the literature on this catalytic system (1–8). Concerning the valence state of vanadium in the active surface, a V^{4+}/V^{5+} equilibrium on the surface of a vanadyl pyrophosphate during *n*-butane oxidation has been demonstrated which is dependent on the time of activation (2, 9, 10).

Our knowledge of the activation of the VPO catalysts has recently been greatly improved due to the use of advanced characterisation techniques, particularly ^{31}P NMR by spin echo mapping (11–13). With the latter technique, it is possible to discriminate different V^{4+} structures surrounding phosphorus atoms depending on their VPO environments. It was demonstrated that the activation of the vanadyl hemihydrate precursor, under the *n*-butane/air stream, proceeded in two parallel routes, either a reoxidation to $VOPO_4$ phases or a direct dehydration to $(VO)_2P_2O_7$. This is followed by a reduction of the residual $VOPO_4$ phases to $(VO)_2P_2O_7$ (13). The kinetics of all these transformations determines the final catalytic performances at the stationary state. It was demonstrated that the best results were associated with a $(VO)_2P_2O_7$ structure in which phosphorus atoms were associated with V^{4+} in a crystalline matrix and with V^{4+} in a disordered matrix together with V^{5+}, implying the importance of V^{4+}–V^{5+} mixed valencies together with the $(VO)_2P_2O_7$ structure (14, 15).

The morphology of the $VOHPO_4, 0.5\,H_2O$ precursor can be changed by following a new route which consists in a reduction of $VOPO_4 \cdot 2\,H_2O$ with isobutanol (16). This latter approach gives a specific morphology of the vanadyl phosphate hemihydrate with extensive development of the crystallites in the [110] direction and limited development in the [001] direction. This corresponds to the production of thin platelets of $VOHPO_4 \cdot 0.5\,H_2O$ preferentially exposing the (001) crystal faces which give, after activation, a large development of the (100) basal face of the $(VO)_2P_2O_7$ crystals and VPO catalysts with higher BET area (16).

In a previous publication we have shown that the $VOPO_4/(VO)_2P_2O_7$ dispersion can be modified by using dopants (17). As examples, Co and Fe dopants were introduced as acetylacetonate salts in isobutanol during the synthesis of the $VOHPO_4 \cdot 0.5\,H_2O$ precursor via the organic route which consists of a reduction of V_2O_5 by isobutanol (18). Doping the bulk structure of the $VOHPO_4 \cdot 0.5\,H_2O$ precursors (19) favoured the nucleation of the $VOPO_4$ structure at a lower temperature and resulted in higher selectivity to MA formation (17).

In the present note, we study the modifications, as determined by ^{31}P NMR by spin echo mapping, which are induced in the physicochemical characteristics of VPO catalysts which have major differences in their morphologies when doped with iron and cobalt at a low percentage (1%) and the correlation with their catalytic performances.

The undoped $VOHPO_4 \cdot 0.5\,H_2O$ precursor, denoted VPO, was prepared by adding V_2O_5 (11.8 g) to isobutanol (250 ml). H_3PO_4 (16.49 g 85%) was then introduced to the mixture which was then refluxed for 16 h. The light blue suspension was then separated from the organic solution by filtration and washed with isobutanol (200 ml) and ethanol (150 ml, 100%). The resulting solid was refluxed in water (9 ml H_2O/g solid), filtered hot, and dried in air (110°C, 16 h).

For the preparation of the two doped 1% Fe/V and Co/V precursors (M = Fe, Co, atomic ratio $V : M = 1 : 0.05$), denoted VPOFe1 and VPOCo1, respectively, the required mass of the corresponding acetylacetonate salts was previously dissolved in isobutanol (according to the atomic M/V stoichiometry), prior to the refluxing operation with isobutanol and 85% H_3PO_4. Further filtration and washing procedures were identical to those used for the undoped precursor. The three VPO precursors were then dried at 120°C in air for 12 h.

The undoped $VOHPO_4 \cdot 0.5\,H_2O$ percursor, denoted VPD, was prepared via $VOPO_4 \cdot 2\,H_2O$ (9). $VOPO_4 \cdot 2\,H_2O$ was prepared from V_2O_5 (12.0 g) and H_3PO_4 (115.5 g 85%) which were refluxed in water (24 ml H_2O/g solid) for 8 h. The resulting $VOPO_4 \cdot 2\,H_2O$ was recovered by filtration and washed with water and finally identified by XRD. Then this solid (4 g) was refluxed with isobutanol (80 ml) for 21 h, and the resulting solid was recovered by filtration and dried in air (110°C, 16 h).

0021-9517/97 $25.00

For the preparation of the two doped 1% Fe/V and Co/V precursors (M = Fe, Co, atomic V : M = 1 : 0.05), denoted VPDFe1 and VPDCo1, respectively, the required mass of the corresponding acetylacetonate salts was previously dissolved in isobutanol (according to the atomic M/V stoichiometry), prior to refluxing $VOPO_4 \cdot 2\ H_2O$ with isobutanol. The subsequent steps in the preparation procedure were followed as for the undoped precursor. The three VPD precursors were then dried at 120°C in air for 12 h.

X-ray diffraction patterns of the materials were recorded with a Siemens diffractometer using Cu K_α radiation. The ^{31}P NMR experiments were performed on a Bruker MSL 300 NMR spectrometer. The ^{31}P spin echo spectra were recorded under static conditions, using a 90°x–τ–180°y–τ–(acquire sequence). The 90° pulse was 4.2 μs and τ was 20 μs. For each sample, the irradiation frequency was varied in increments of 100 kHz above and below the ^{31}P resonance of H_3PO_4. The number of spectra thus recorded was dictated by the frequency limits beyond which no spectral intensity was visible. The ^{31}P NMR spin echo mapping information was then obtained by juxtaposition of each experimental spectrum. Surface area was determined by the BET method using nitrogen gas at liquid nitrogen temperature.

The oxidation of *n*-butane was carried out using a microreactor working under differential conditions with 1 cm^3 of the precursor and the feedstock composition $C_4H_{10}/O_2/He = 1.5/18.5/80$, GSHV = 1000 h^{-1}. The activation of the precursors was performed over a period of 25 h at 430°C, and the catalysts were then cooled at room temperature under the reaction atmosphere. Maleic anhydride (MA) was the main product detected, together with traces of butadiene and furan. Detection of reactants and products was performed on line by gas chromatography with good carbon mass balances (98–100%).

Chemical analysis showed that Co and Fe are present in the two $VOHPO_4 \cdot 0.5\ H_2O$ structures with the expected Co/V and Fe/V atomic ratios (1.0%) for both VPO and the VPD series. A STEM-EDX examination of the four doped precursors showed a homogeneous dispersion of Co and Fe dopants in the hemihydrate platelets (19).

The XRD spectra of the VPO doped precursors showed that doping with low concentration affects the peak structure for the VPO series (the effect of Fe appears to be more marked), while, in contrast, significant modification was observed for the doped VPD series, particularly in the case of doping by Fe. The modification of the structure induced by doping with Co or Fe was in agreement with the variation of the BET area (Table 1). While these values are almost unchanged for the VPO precursors, a strong decrease is observed for the VPD precursors, particularly when doping with Fe. A SEM examination confirmed, in this case, that the morphology with the (001) platelets highly developed for VPD was markedly affected. The ^{31}P NMR spectra by spin echo mapping of the doped precursors were all similar with a characteristic signal at 1625 ppm, as previously observed (12), which confirmed a good dispersion of the two dopants.

TABLE 1

BET Area of the Doped VPO Precursors and Catalysts as Compared to the Undoped Standards

Precursors	S_{BET} (m^2/g)	Catalysts	S_{BET} (m^2/g)
VPO	11.0	VPOac	13.0
VPOCo1	9.1	VPOCo1ac	16.3
VPOFe1	7.1	VPOFe1ac	18.8
VPD	32.0	VPDac	42.4
VPDCo1	22.9	VPDCo1ac	50.4
VPDFe1	10.1	VPDFe1ac	13.3

Figures 1 and 2 show the evolution of the catalytic performance at 430°C for catalysts of the VPO and VPD series, respectively, as shown from the variation of selectivity versus *n*-butane conversion (numbers near the experimental points correspond to different times of activation expressed in hours). Selectivity to maleic anhydride (S_{MA}) increases with *n*-butane conversion (C_{But}), but the effect of doping differs when considering the two series.

For the VPO series (Fig. 1), the favourable effect of doping appears after a long time of activation. This is obvious when comparing the same *n*-butane conversion of 60%: it appears that the undoped VPO needs 43 h of activation, S_{MA} being 56%, while Co-doped VPO needs 20 h (S_{MA} being 80%), and Fe-doped VPO needs only 10 h (S_{MA} being

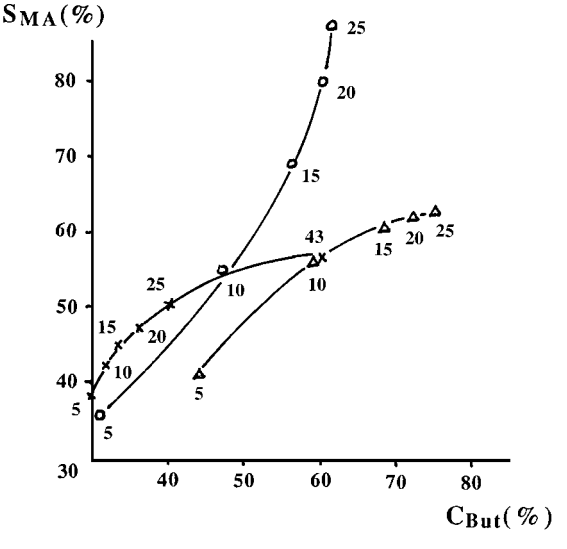

FIG. 1. Catalytic performance at 430°C of the vanadium phosphorus oxide catalysts (VPO route) as a function of the time of activation ($C_4H_{10}/O_2/He = 1.5/18.5/80$, GSHV = 1000 h^{-1}): (×) VPO, reference catalyst; (○) VPOCo1; Co doped (Co/V = 1%); (△) VPOFe1, Fe doped (Fe/V = 1%). C_{But} is the *n*-butane conversion; S_{MA} the selectivity to maleic anhydride. Small numbers correspond to the time of activation in hours.

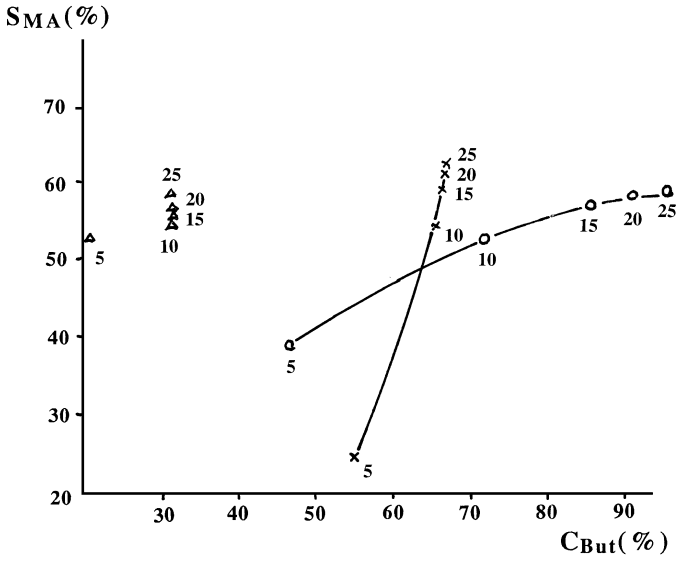

FIG. 2. Catalytic performance at 430°C of the vanadium phosphorus oxide catalysts (VPD route) as a function of the time of activation ($C_4H_{10}/O_2/He = 1.5/18.5/80$, GSHV = 1000 h^{-1}): (×) VPD, reference catalyst; (○) VPDCo1, Co doped (Co/V = 1%); (△) VPDFe1, Fe doped (Fe/V = 1%). C_{But} is the *n*-butane conversion; S_{MA} the selectivity to maleic anhydride. Small numbers correspond to the time of activation in hours.

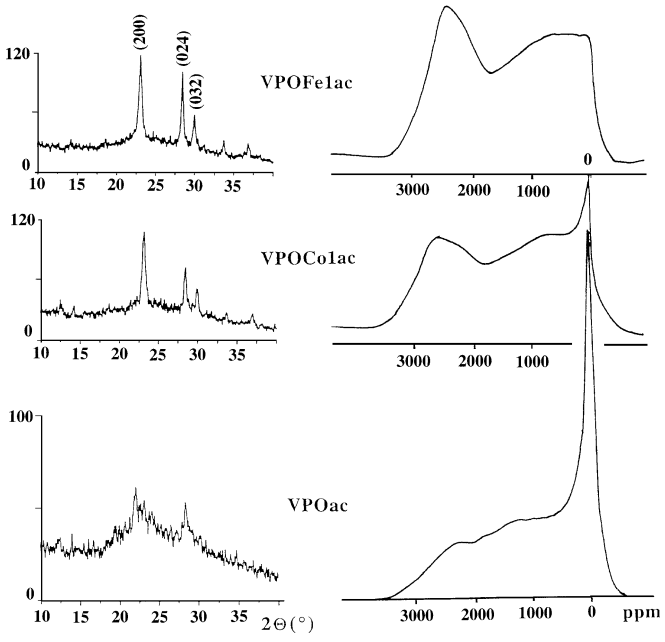

FIG. 3. XRD spectra and ^{31}P spin echo mapping spectra of the vanadium phosphorus oxide catalysts after catalysis (VPO route): VPOac, reference catalyst; VPOCo1ac, Co doped (Co/V = 1%); VPOFe1ac, Fe doped (Fe/V = 1%).

56%). Co and Fe dopants also lead to a small increase in the final surface area of the catalysts (Table 1).

For the VPD series, the favourable effect of doping appears only for Co; indeed, 60% *n*-butane conversion is reached after 7 h of activation for the undoped-VPD (S_{MA} being only 35%), while Co-doped VPD needs 8 h (S_{MA} being 47%). We have not found it possible to reach such a high conversion even after a long time of activation in the case of Fe-doped VPD. With this catalyst it is difficult to exceed 32% *n*-butane conversion, which indicates that in this case there is a limitation of the active area. This is confirmed from the values of the BET area (Table 1) (while it has been increased for Co-doped VPO (50.4 m^2/g), a marked decrease is observed for Fe-doped VPD (13.3 m^2/g) as compared to 42.4 m^2/g for undoped VPD). From the literature data, it is well known that a high BET area of the vanadium phosphorous oxides catalyst is generally associated with a high development of the basal (100) $(VO)_2P_2O_7$ face and this is the interesting feature of the VPD catalyst. There is a limitation of the MA selectivity around 60% for the VPD series, but with very different *n*-butane conversion (67% for undoped VPD, 25 h of activation; 95% for Co-doped VPD, 25 h of activation; and 32% for Fe-doped VPD, 25 h of activation).

Figure 3 shows the XRD spectra (Fig. 3a) and the ^{31}P NMR spin echo mapping spectra (Fig. 3b) of the series of VPO catalysts after the catalytic test. The undoped VPO catalyst is poorly crystalline. The ^{31}P NMR spectrum by spin echo mapping shows three signals; (i) at 0 ppm (P atoms connected to V^{5+} in the $VOPO_4$ phases); (ii) at 2400 ppm (P atoms connected to V^{4+} in the poorly crystallized $(VO)_2P_2O_7$ phase); and (iii) in the 200–1500 ppm range (which has previously been attributed to P atoms connected to V^{4+}–V^{5+} dimers in a poorly crystalline $(VO)_2P_2O_7$ matrix (12–14)). Table 2 gives the relative distribution of these three species for the VPO catalyst series, evaluated from spectra shown in Fig. 3b (see Ref. (13)).

The VPOCo1 and VPOFe1 catalysts show the characteristic (200), (024), and (032) XRD reflections of $(VO)_2P_2O_7$ at 23, 28.45, and 29.9° 2Θ, respectively. These doped catalysts appear to be more crystalline as compared to the undoped VPO catalyst. Such observations are consistent with the ^{31}P NMR spectra by spin echo mapping which show an increase of the contribution of the signal at 2400 ppm attributed to crystalline $(VO)_2P_2O_7$ for these two catalysts

TABLE 2

Distribution of the Vanadium Species as Evaluated from the Spectra of ^{31}P NMR by Spin Echo Mapping (See Ref. (13))

Catalysts	V^{4+}(%) (signal at 2400 ppm)	V^{4+}–V^{5+}(%) (signal at 200–1500 ppm)	V^{5+}(%) (signal at 0 ppm)
VPOac	20.3	45.4	34.3
VPOCo1ac	30.8	53.9	16.3
VPOFe1ac	40.0	53.2	6.8
VPDac	76.0	20.0	4.0
VPDCo1ac	80.2	16.6	3.2
VPDFe1ac	26.0	55.1	18.9

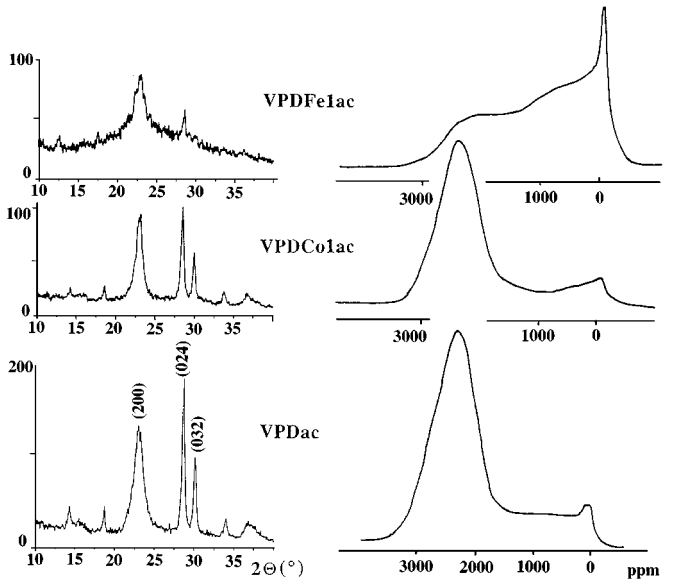

FIG. 4. XRD spectra and ^{31}P spin echo mapping spectra of the vanadium phosphorus oxide catalysts after catalysis (VPD route): VPDac, reference catalyst; VPDOCo1ac, Co doped (Co/V = 1%); VPDFe1ac, Fe doped (Fe/V = 1%).

together with a decrease of the signal at 0 ppm due to the $VOPO_4$ phases. It is apparent, from Fig. 3b and Table 2, that the signal due to V^{4+}–V^{5+} dimers in the 200–1500 ppm range has also increased.

Figure 4 shows the XRD spectra (Fig. 4a) and the ^{31}P NMR spin echo mapping spectra (Fig. 4b) of the series of VPD catalysts after the catalytic test. While the VPD and VPDCo1 catalysts appear characteristic of well crystallized $(VO)_2P_2O_7$, VPDFe1 is poorly crystalline with the three signals observed by ^{31}P NMR spin echo mapping which demonstrate the presence of $VOPO_4$ phases (0 ppm), crystallized $(VO)_2P_2O_7$ (2400 ppm) and poorly crystalline $(VO)_2P_2O_7$ (200–1500 ppm). Table 2 shows that, in the VPDFe1 case, the contribution of the V^{4+}–V^{5+} dimers is highly important (55.1%) (but almost in the absence of crystallized $(VO)_2P_2O_7$), whereas this contribution is much lower for the VPDCo1 and VPD catalysts (16.6 and 20.0%, respectively).

A significant improvement of the catalytic performance is observed for the *n*-butane conversion and for the selectivity to maleic anhydride when doping the VPO precursor with both Co and Fe. This effect is pronounced for a long time of activation. A comparable effect is observed only for the VPD series when doped with Co. In this latter case, the promoting effect is observed for the *n*-butane conversion. This can be correlated with the increase of the BET area connected to the development of the (100) basal crystal face of $(VO)_2P_2O_7$. Doping leads to changes in the microstructure of the vanadium phosphorus oxide catalysts as indicated by XRD and ^{31}P NMR spin echo mapping. Two previous studies of the activation of the VPO (17) and VPD (20) precursors by *in situ* Raman spectroscopy have shown that the two dopants both promote the nucleation of the $VOPO_4$ phases in the first period of the activation process which changes the kinetics of the three steps (oxidation–dehydration–reduction) that occur during the activation of the precursor, principally by accelerating the oxidation step. This changes the V^{5+}/V^{4+} balance throughout this transformation period as shown by Raman spectroscopy and XPS (20) and influences the catalytic performance. By using ^{31}P NMR spin echo mapping, the present study has shown that the microstructure of the vanadium phosphorus oxide catalyst is altered by the dopant and that this effect differs depending on its nature and on the preparation conditions of the precursor. For the activated VPO catalyst, doping with Co and Fe both leads primarily to the formation of $(VO)_2P_2O_7$ as a disorganized and crystallized structure which tends to strongly improve the catalytic performance. In the case of the activated VPD catalyst, Fe causes the $(VO)_2P_2O_7$ to exist as a poorly crystalline structure, and this explains the poor performances of this catalyst. On the other hand, Co generates significantly crystalline $(VO)_2P_2O_7$ together with a poorly crystalline $(VO)_2P_2O_7$ structure, a combination that gives enhanced catalytic performance. It appears that the best catalytic performances can be correlated with the presence of these two structures with V^{4+} cations and V^{4+}–V^{5+} dimers.

^{31}P NMR by spin echo mapping can be used to provide an estimate of these different P environments with the signals at 2400 ppm and 200–1500 ppm, respectively, and to evaluate their respective role in the catalytic performances. In Fig. 5, the intrinsic activity for the MA formation has

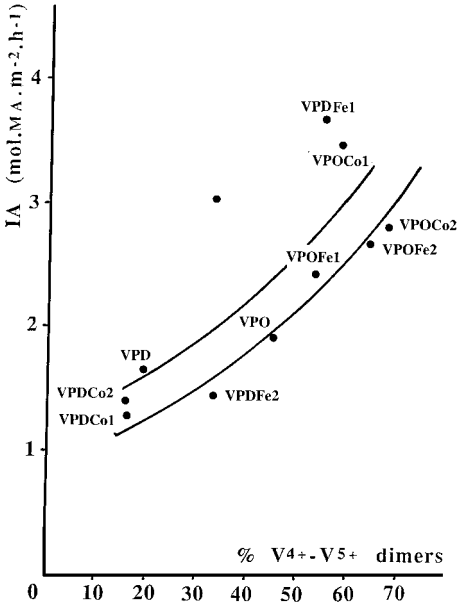

FIG. 5. Correlation between the intrinsic activity for MA formation and the contribution of the V^{4+}–V^{5+} dimers (200–1500 ppm) evaluated from the ^{31}P NMR spin echo mapping spectra (see Table 2).

been plotted versus the intensity of the signal at 200–1500 ppm attributed to V^{4+}–V^{5+} dimers for the VPO, VPOCo1, VPOFe1, VPD, VPDCo1, and VPDFe1 catalysts considered in this study. Results have also been added for catalysts VPOCo2, VPOFe2, VPDCo2, and VPDFe2, corresponding to 2% doping by Co and Fe, although the detailed results for these catalysts are not presented here. A clear correlation is observed which stresses the importance of the V^{4+}–V^{5+} dimers in controlling the catalytic activity for *n*-butane oxidation to maleic anhydride. Indeed, the specific activity of the catalysts increases with increasing concentration of V^{4+}–V^{5+} dimers. This situation is always associated with the presence of crystalline $(VO)_2P_2O_7$. The correlation between specific activities and the concentration of V^{4+}–V^{5+} dimers is consistent with a recent study of vanadium phosphorus oxide catalysts prepared by the aqueous HCl method where a correlation between specific activity and the fraction of $VOPO_4$ present in the catalysts (21) shows a similar relationship to the correlation shown in Fig. 5. It is therefore considered that the results of this study have general applicability to vanadium phosphorus oxide catalysts. It demonstrates that $(VO)_2P_2O_7$ alone is not the active phase for selective oxidation of *n*-butane to maleic anhydride, but that a suitable V^{4+}/V^{5+} balance is required for the best performance on this matrix. This study has demonstrated that doping can change this balance with time of activation. The effect is however very complex since it depends on the nature of the dopant (influence of the redox potential) and on the preparation conditions of the corresponding precursors.

ACKNOWLEDGMENTS

The authors are indebted to the European Human Capital and Mobility Programme (Contract CHRX-CT92-0065) for financial support.

REFERENCES

1. Centi, G. (Ed.), "Vanadyl Pyrophosphate Catalysts," Catalysis Today, Vol. 16, No. 1, Elsevier, Amsterdam, 1993.
2. Centi, G., Trifiro, F., Ebner, J. R., and Franchetti, V. M., *Chem. Rev.* **88**, 55 (1988).
3. Udovich, C. A., and Edwards, R. C., U.S. Patent 4,564,688 (to Amoco), 1986.
4. Barone, B. J., Europeon Patent 458,541 (1981); U. S. Patent 5,070,060 assigned to Scientific Design Co.
5. Schneider, R. A., U.S. Patent 4043943 (assigned to Chevron), 1977.
6. Ebner, J. R., U.S. Patent 185,455 (assigned to Monsanto Co.), 1993.
7. Mc Dermott, J. X., German Offen 2,834,554 (assigned to Halcon Co.), 1979.
8. Barone, B. J., U.S. Patent 5,158,923 (assigned to Scientific Design Co.), 1992.
9. Hodnett, B. K., *Catal. Today* **1**, 477 (1987).
10. Zhang, Y., Sneeden, R. P. A., and Volta, J. C., *Catal. Today* **16**, 39 (1993).
11. Li, J., Lashier, M. E., Schrader, G. L., and Gerstein, B. C., *Appl. Catal.* **73**, 83 (1991).
12. Sananés, M. T., Tuel, A., and Volta, J. C., *J. Catal.* **145**, 251 (1994).
13. Abon, M., Bere, K. E., Tuel, A., and Delichere, P., *J. Catal.* **156**, 28 (1995).
14. Lopez Granados, M., Conesa, J. C., and Fernandez-Garcia, M., *J. Catal.* **141**, 671 (1993).
15. Sananés, M. T., Tuel, A., Hutchings, G. J., and Volta, J. C., *J. Catal.* **148**, 395 (1994).
16. Hutchings, G. J., Olier, R., Sananés, M. T., and Volta, J. C., *in* "New Developments in Selective Oxidation" (V. Cortés Corberan and S. Vic Bellon, Eds.), Studies in Surface Science, Vol. 82, p. 213, Elsevier, Amsterdam, 1994.
17. Ben Abdelouahab, F., Olier, R., Ziyad, M., and Volta, J. C., *J. Catal.* **157**, 687 (1995).
18. Johnson, J. W., Johnston, D. C., Jacobson, A. J., and Brody, J. F., *J. Am. Chem. Soc.* **106**, 8123 (1984).
19. Ben Abdelouahab, F., Ziyad, M., Leclercq, C., Millet, J. M., Olier, R., and Volta, J. C., *J. Chim. Phys.* **92**, 1320 (1995).
20. Sananés, M. T., Ben Abdelouahab, F., Hutchings, G. J., and Volta, J. C., *J. Catal.*, in press.
21. Hutchings, G. J., and Higgins, R., *J. Catal.*, in press.

M. T. Sananes-Schulz*,†
A. Tuel*
G. J. Hutchings†
J. C. Volta*

**Institut de Recherches sur la Catalyse*
CNRS, 2 Avenue A. Einstein
69626, Villeurbanne Cédex, France
†*Leverhulme Centre for Innovative Catalysis*
Department of Chemistry
University of Liverpool, P.O. Box 147
Liverpool, L69 3BX, United Kingdom

Received June 26, 1996; revised October 3, 1996; accepted November 4, 1996